Thermo-physical properties of body-centered cubic iron-magnesium alloys under extreme conditions

K. Kádas[a,b], R. Ahuja[a,c], B. Johansson[a,c], O. Eriksson[c], L. Vitos[a,b,c]

[a] *Applied Materials Physics, Department of Materials Science and Engineering, The Royal Institute of Technology SE-10044 Stockholm, Sweden*
[b] *Research Institute for Solid State Physics and Optics, H-1525 Budapest, P.O.Box 49, Hungary*
[c] *Materials Theory, Department of Physics and Astronomy, Uppsala University, Box 516, SE-751 20, Uppsala, Sweden*

Abstract

Using density functional theory formulated within the framework of the exact muffin-tin orbitals method, we investigate the thermo-physical properties of body-centered cubic (bcc) iron-magnesium alloys, containing 5 and 10 atomic % Mg, under extreme conditions, at high pressure and high temperature. The temperature effect is taken into account via the Fermi-Dirac distribution of the electrons. We find that at high pressures pure bcc iron is dynamically unstable at any temperature, having a negative tetragonal shear modulus (C'). Magnesium alloying significantly increases C' of Fe, and bcc Fe-Mg alloys become dynamically stable at high temperature. The electronic structure origin of the stabilization effect of Mg is discussed in details. We show that the thermo-physical properties of a bcc Fe-Mg alloy with 5% Mg agree well with those of the Earth's inner core as provided by seismic observations.

Keywords: Ab initio, Fe-alloys, elasticity, dynamical stability, Earth's inner core

1. Introduction

Despite very intense research efforts, the structure and the composition of the Earth's solid inner core is still unknown. It is widely accepted, that iron is its main component, however there is no consensus about the crystal phase in which iron is present. In recent years, Fe was suggested to occur in the core in the body-centered cubic (bcc) phase [1, 2, 3, 4, 5]. It is known, however, that the density of pure Fe is larger than that of the inner core. Consequently, one or more light elements are necessarily present in the core beyond Fe. Bcc Fe-based composition models containing silicon [6, 7], sulphur [7], and nickel [8] alloying elements can reproduce the density deficit [9] of the inner core. However, none of these composition models show agreement in other physical properties of the inner core, as given in the Preliminary Reference Earth Model [10]. We have suggested earlier that magnesium, one of the most abundant of Earth elements, is a strong candidate light element of the inner core [11, 12].

The partition of Mg into the inner core is still controversial [11]. Mg is often classified as a litophile element [13, 14], and therefore its presence in the core is precluded. This is based on two main arguments. First, the consistency between the relative amount of Mg in the Earth's mantle and in the chondritic models, led to the thought that the occurrence of Mg in the core is unlikely. Second, based on oxygen fugacity at mantle conditions [15], metallic Mg in the core is believed to require extremely reducing conditions. However, the oxygen fugacity significantly increases with increasing temperature for Mg, indicating that at inner core conditions the presence of Mg can not be ruled out [15]. Furthermore, the ionic character of metal oxides at the

extreme conditions of the core, is not yet understood.

Here, without examining the partition of Mg into the core, we analyze the thermo-physical properties of bcc Fe-Mg alloys up to core conditions, and give an electronic structure explanation of their dynamical stability. We note that the thermodynamic stability is not discussed in this study.

The paper is organized as follows. In Section 2 we briefly review the computational details of the theoretical calculations. In Section 3 we present the equation of state for bcc Fe and Fe-Mg alloys containing 5 and 10% Mg, the single crystal elastic constants at zero and at high (T=7000 K) temperature, and the polycrystalline elastic constants of the alloys. Next, based on electronic structure analysis, we explain the dynamical stability of pure bcc Fe and Fe-Mg alloys. Finally, we compare the thermo-physical properties of bcc Fe-Mg alloys considered here with those of the Earth's inner core.

2. Computational details

The present ab initio calculations are based on density functional theory [16] using the generalized gradient approximation (GGA) [17] for the exchange-correlation functional. The Kohn-Sham equations were solved using the Exact Muffin-tin Orbitals method [18, 19, 20, 21]. This scheme was proved to be an accurate approach in the theoretical description of the disordered solid solutions [20, 22, 23, 24]. Non-magnetic calculations were done to determine the elastic constants, since bcc Fe and Fe-Mg alloys are non-magnetic at inner core conditions [12]. The two cubic shear constants, $C' = (C_{11} - C_{12})/2$ and C_{44}, were obtained from volume-conserving

orthorhombic and monoclinic distortions, as in Refs. [12, 25]. The temperature dependence of the elastic constants was calculated for T=7000 K as described in Ref. [26].

3. Results and discussion

We calculated the equation of state for pure bcc Fe, as well as for bcc $Fe_{1-x}Mg_x$ ($Fe_{0.95}Mg_{0.05}$ and $Fe_{0.9}Mg_{0.1}$) alloys at zero temperature (Fig. 1). For comparison, for pure Fe both the nonmagnetic (NM) and ferromagnetic (FM) states were considered. (The numerical details of the FM calculations are similar to the NM ones.) Figure 1 shows that the volumes of NM and FM bcc Fe are notably different at low pressure, but the volume difference gradually decreases with increasing pressure and disappears around ≈300 GPa. This is in line with the gradually vanishing calculated ferromagnetic moment on Fe.

The effect of Mg-alloying can be observed in Fig. 1. At low pressures, the volume of Fe-Mg alloys increases with the Mg content. This can be explained with the larger atomic size of Mg: its metallic atomic radius is 27% larger than that of Fe. The change in volume with increasing Mg concentration decreases with increasing pressure, which can be understood by considering that Mg has a significantly higher compressibility, than Fe [27]. The volume difference between pure Fe and Fe-Mg alloys practically vanishes at core pressures (329-364 GPa [10]).

The zero temperature shear elastic constants, C', C_{44}, and the bulk modulus, B, calculated at different V volumes for for pure bcc Fe, $Fe_{0.95}Mg_{0.05}$ and $Fe_{0.9}Mg_{0.1}$ alloys are shown in Table 1). At T=0 K, pure bcc Fe is dynamically

unstable, since one of its elastic constants, the tetragonal shear modulus (C') is negative at each volume. In addition, C' shows an anomalous behavior: it increases with increasing volume. However, C' remains negative at each volume, even in $Fe_{0.9}Mg_{0.1}$. We calculate $(\Delta C'/\Delta V)_{Fe}$=7.6 GPa/Bohr^3 for pure iron, and $(\Delta C'/\Delta V)_{Fe_{0.95}Mg_{0.05}}$=4.1 GPa/Bohr^3 and $(\Delta C'/\Delta V)_{Fe_{0.9}Mg_{0.1}}$=1.7 GPa/Bohr^3 for the alloys. For each volume, C' strongly increases with increasing Mg concentration. $\Delta C'/\Delta x$ decreases with increasing volume: $\Delta C'/\Delta x$=2018.9 GPa/a.f. at V=44.60 Bohr^3/atom reduces to $\Delta C'/\Delta x$=123.1 GPa/a.f. at V=59.91 Bohr^3/atom volume, where a.f. stands for atomic fraction.

C_{44} follows a normal decreasing behavior with increasing volume (Table 1). We obtain $(\Delta C_{44}/\Delta V)_{Fe}$=-27.5 GPa/Bohr^3, $(\Delta C_{44}/\Delta V)_{Fe_{0.95}Mg_{0.05}}$=-26.0 GPa/Bohr^3, and $(\Delta C_{44}/\Delta V)_{Fe_{0.9}Mg_{0.1}}$=-23.8 GPa/Bohr^3. C_{44} diminishes with increasing Mg concentration, and $|\Delta C_{44}/\Delta x|$ decreases with increasing volume: we calculate $\Delta C_{44}/\Delta x$=-1031.8 GPa/a.f. at V=44.60 Bohr^3/atom, and $\Delta C_{44}/\Delta x$=-541.1 GPa/a.f. at V=59.91 Bohr^3/atom volume.

The bulk modulus decreases normally with increasing volume (Table 1), the changes being $(\Delta B/\Delta V)_{Fe}$=-62.4 GPa/Bohr^3, $(\Delta B/\Delta V)_{Fe_{0.95}Mg_{0.05}}$=-59.6 GPa/Bohr^3, and $(\Delta B/\Delta V)_{Fe_{0.9}Mg_{0.1}}$=-57.1 GPa/Bohr^3. B diminishes with increasing Mg concentration, and the change due to Mg alloying is significantly smaller at larger volumes: $\Delta B/\Delta x$=-768 GPa/a.f. at V=44.60 Bohr^3/atom reduces to $\Delta B/\Delta x$=-60 GPa/a.f. at V=59.91 Bohr^3/atom volume.

The dynamical instability of bcc Fe and Fe-Mg alloys can be understood from their electronic structure. The most important change in DOS can be

seen at the Fermi level (E_{F}), where the large peak in pure Fe is significantly decreased by doping. In Fig. 2 we show how the DOS changes in bcc Fe and $Fe_{0.9}Mg_{0.1}$, upon orthorhombic distortion δ, which was used to compute C'. In bcc Fe, this distortion splits the degenerated d peak located around -7 mRy below E_{F}. This peak corresponds mainly to e_g states. On splitting one d subband is pushed toward negative energies, and one d subband is moved above E_{F}. The DOS below E_{F}, between -0.06 Ry and 0 Ry decreases significantly (Fig. 2, black striped area). This splitting, and the corresponding decrease in DOS gives a notable negative contribution to the electronic energy. Consequently, the total energy of bcc Fe decreases upon lattice distortion, resulting in a large negative tetragonal shear constant. Indeed, we calculate C'=-285.3 GPa for bcc Fe at zero temperature and V=44.60 Bohr^3/atom volume. This mechanism is responsible for the dynamical instability of bcc Fe at high pressures and low temperatures. Magnesium alloying significantly reduces the above effect. Due to the chemical disorder, the DOS is much smoother near E_{F} in $Fe_{0.9}Mg_{0.1}$ (Fig. 2, solid red line) than in pure Fe. This results in that the energy decrease upon lattice distortion is much smaller in $Fe_{0.9}Mg_{0.1}$ (Fig. 2, red striped area) than in pure Fe. Accordingly, the alloy is still unstable dynamically, but its tetragonal shear constant is larger than that of pure Fe. Indeed, we calculate C'=-83.4 GPa for $Fe_{0.9}Mg_{0.1}$ at zero temperature and V=44.60 Bohr^3/atom volume.

In the following we examine the elastic constants at T=7000 K (Table 1). At this temperature, pure bcc Fe is in our calculations still unstable at high pressures, i.e. at small volumes. Namely, at V=44.60 Bohr^3/atom, we calculate C'=-43.7 GPa for Fe at T=7000 K (Table 1). Similarly to the

zero temperature anomalous behavior, C' increases with increasing volume at T=7000 K in both pure Fe and $Fe_{0.95}Mg_{0.05}$, but to a lower extent than at zero temperature [$(\Delta C'/\Delta V)_{Fe}$=4.1 GPa/Bohr^3, $(\Delta C'/\Delta V)_{Fe_{0.95}Mg_{0.05}}$=1.6 GPa/Bohr^3]. In $Fe_{0.9}Mg_{0.1}$, C' follows a normal decreasing behavior with increasing volume, $(\Delta C'/\Delta V)_{Fe_{0.9}Mg_{0.1}}$ being -0.6 GPa/Bohr^3. In pure bcc Fe, C' becomes positive at V=54.36 Bohr^3/atom. At this temperature, Mg alloying dynamically stabilizes bcc Fe. We calculate positive C' at each volume in both Fe-Mg alloys. At V=44.60 Bohr^3/atom, C'=8.8 GPa for $Fe_{0.95}Mg_{0.05}$, and C'=55.14 GPa for $Fe_{0.9}Mg_{0.1}$. The increasing Mg content increases C', but to a lower extent than at zero temperature. $\Delta C'/\Delta x$=988.5 GPa/a.f. at V=44.60 Bohr^3/atom, which is less than half of that at T=0 K. $\Delta C'/\Delta x$ decreases with increasing volume: at V=59.91 Bohr^3/atom volume we obtain $\Delta C'/\Delta x$=351.5 GPa/a.f.

C_{44} decreases with increasing volume in both pure Fe and in Fe-Mg alloys at T=7000 K (Table 1). $|\Delta C_{44}/\Delta V|$ is slightly smaller at this high temperature, compared to those at T=0 K. At T=7000 K we obtain $(\Delta C_{44}/\Delta V)_{Fe}$=-26.0 GPa/Bohr^3, $(\Delta C_{44}/\Delta V)_{Fe_{0.95}Mg_{0.05}}$=-24.2 GPa/Bohr^3, and $(\Delta C_{44}/\Delta V)_{Fe_{0.9}Mg_{0.1}}$=-22.5 GPa/Bohr^3. C_{44} decreases with increasing Mg concentration at each V volume, but to a lower extent than at zero temperature. We calculate $\Delta C_{44}/\Delta x$=-629.7 GPa/a.f. at V=44.60 Bohr^3/atom, and $C_{44}/\Delta x$=-165.7 GPa/a.f. at V=59.91 Bohr^3/atom volume.

The bulk modulus, B, decreases with increasing volume in both pure bcc Fe and in the alloys at high temperature (Table 1), approximately to the same extent as at T=0 K ($(\Delta B/\Delta V)_{Fe}$=-63.1 GPa/Bohr^3, $(\Delta B/\Delta V)_{Fe_{0.95}Mg_{0.05}}$=-60.4 GPa/Bohr^3, $(\Delta B/\Delta V)_{Fe_{0.9}Mg_{0.1}}$=-57.8 GPa/Bohr^3). B decreases with

increasing Mg concentration at each V volume. The high temperature bulk moduli are slightly larger than those calculated at zero temperature, and $\Delta B/\Delta x$ is approximately the same as those at T=0 K at each V volume. We obtain $\Delta B/\Delta x$=-778 GPa/a.f. at V=44.60 Bohr^3/atom, and $\Delta B/\Delta x$=-70 GPa/a.f. at V=59.91 Bohr^3/atom volume.

The electronic entropy is proportional to the DOS at the Fermi level, when the DOS varies slowly with E near $E_{\rm F}$ [28]. Comparing the DOS around $E_{\rm F}$ for pure bcc (Fig. 2) and hcp (hexagonal closed packed) Fe (Fig. 2 in Ref. [12]), we can observe that (i) the DOS at $E_{\rm F}$ is significantly larger in the bcc phase, and (ii) the DOS is more irregular in bcc Fe compared to the almost constant DOS calculated for the hcp phase. These changes in the DOS result in that the electron excitations are more significant in the case of the bcc structure than for the hcp structure. The increasing temperature increases C' of bcc Fe, first of all because the electronic entropy increases with distortion. In bcc Fe at T=7000 K, the electronic entropy term in the Gibbs free energy (-$TS_{\rm e}$) is 3.0 mRy larger in the distorted structure than in the non-distorted system. In $Fe_{0.9}Mg_{0.1}$, -$TS_{\rm e}$ is increased by 1.6 mRy in the distorted structure compared to that of the non-distorted system. This shows that the dynamical stabilization effect of temperature is larger in pure Fe than in Fe-Mg alloys. However, this can not compensate the large chemical stabilization effect of Mg, which is present already at low temperatures (we recall that at T=0 K and V=44.60 Bohr^3/atom we obtain C'=-285.24 GPa for Fe, and C'=-83.38 GPa for $Fe_{0.9}Mg_{0.1}$). Accordingly, at T=7000 K and V=44.60 Bohr^3/atom, we calculate C'=-43.71 GPa for pure bcc Fe, and C'=55.14 GPa for $Fe_{0.9}Mg_{0.1}$.

The polycrystalline shear modulus (G) is not defined for dynamically unstable systems. Accordingly, in the following, we examine the polycrystalline elastic constants at T=7000 K temperature, for the dynamically stable bcc Fe-Mg alloys, and reveal the effect of Mg alloying on the elastic properties. The Hashin-Shtrikman averages [29] of the shear modulus (G), the Young modulus (E), the polycrystalline anisotropy (A), and the longitudinal ($v_{\rm P}$) and transversal ($v_{\rm S}$) sound velocities calculated for bcc $Fe_{0.95}Mg_{0.05}$ and $Fe_{0.9}Mg_{0.1}$ alloys at different volumes and at T=7000 K are shown in Table 2. The shear modulus follows a normal decreasing behavior with increasing volume in both alloys. Between V=44.60 and V=57.91 Bohr^3/atom G decreases by 20% in $Fe_{0.95}Mg_{0.05}$, and 39% in $Fe_{0.9}Mg_{0.1}$. The shear modulus increases with Mg alloying at each volume considered here. The change in G, due to the increased Mg content, diminishes with increasing volume. This is because G decreases almost linearly with increasing volume in $Fe_{0.9}Mg_{0.1}$, while in $Fe_{0.95}Mg_{0.05}$ $|\Delta G/\Delta V|$ increases with increasing volume. G is 49% larger in $Fe_{0.9}Mg_{0.1}$ than in $Fe_{0.95}Mg_{0.05}$ at V=44.60 Bohr^3/atom, and the corresponding difference in G is only 15% at V=57.91 Bohr^3/atom.

Magnesium enhances the stiffness of bcc Fe at T=7000 K, as the Young moduli, $E = 9BG/(3B + G)$, are higher in $Fe_{0.9}Mg_{0.1}$ than in $Fe_{0.95}Mg_{0.05}$ at each volume (Table 2). In $Fe_{0.9}Mg_{0.1}$, E decreases approximately linearly with increasing volume (i.e. with decreasing pressure), while in $Fe_{0.95}Mg_{0.05}$ $|\Delta E/\Delta V|$ increases with increasing volume. Because of this, the change in E due to 5% Mg addition diminishes with increasing volume: E is 47% larger in $Fe_{0.9}Mg_{0.1}$ than in $Fe_{0.95}Mg_{0.05}$ at V=44.60 Bohr^3/atom, and this difference is reduced to 14% at V=57.91 Bohr^3/atom.

In polycrystalline materials, $A = (G_{\rm V} - G_{\rm R})/(G_{\rm V} + G_{\rm R})$ can be used as a measure of elastic anisotropy, where $G_{\rm V}$ and $G_{\rm R}$ are the Voight and Reuss shear moduli [28]. In an isotropic material, the Voight and Reuss averages of the shear moduli are equal, so that A=0. The more anisotropic a material is, the larger A value it has. The bcc Fe-Mg alloys considered here are highly anisotropic: A varies between 0.90 and 0.51 in $Fe_{0.95}Mg_{0.05}$, and it changes between 0.53 and 0.37 in $Fe_{0.9}Mg_{0.1}$ (Table 2). The anisotropy is larger in $Fe_{0.95}Mg_{0.05}$ than in $Fe_{0.9}Mg_{0.1}$ at each volume, indicating that the increasing Mg content decreases the anisotropy of the alloys. For both alloys the anisotropy decreases with increasing volume. As a comparison, we note, that there is a significant difference in anisotropy between the two phases, namely the bcc and hcp phases of pure Fe. Hexagonal Fe is almost isotropic: A=0.02 at V=44.60 Bohr^3/atom [11]. In this phase, Mg alloying does not change anisotropy notably: at the same V=44.60 Bohr^3/atom volume, A=0.03 in hcp $Fe_{0.95}Mg_{0.05}$, and A=0.04 in hcp $Fe_{0.9}Mg_{0.1}$.

The longitudinal sound velocity, $v_{\rm P} = \sqrt{\frac{B+4G/3}{\varrho}}$ (ϱ being the density), decreases linearly with increasing volume (Table 2) in both $Fe_{0.95}Mg_{0.05}$ and $Fe_{0.9}Mg_{0.1}$. Since $B \gg G$ in these alloys, we find that $v_{\rm P} \sim \sqrt{B}$, which in turn follows a linear trend with volume. Increasing Mg content raises $v_{\rm P}$ at each V volume. The transversal sound velocity, $v_{\rm S} = \sqrt{G/\varrho}$, monotonically decreases with increasing volume in $Fe_{0.9}Mg_{0.1}$ (Table 2). In $Fe_{0.95}Mg_{0.05}$, $v_{\rm S}$ follows a different behavior: it increases with increasing volume up to V=50.97 Bohr^3/atom, and decreases above V=54.36 Bohr^3/atom. The trend in $v_{\rm S}$ vs. volume obtained for $Fe_{0.95}Mg_{0.05}$ and $Fe_{0.9}Mg_{0.1}$ can be explained by $v_{\rm S}$ being approximately proportional to $\sqrt{G}$ in bcc Fe-Mg alloys. The

transversal sound velocity is raised by increasing Mg content at each volume.

Iron-based alloys at high pressure and temperature are relevant to the Earth's solid inner core. Physical properties of the core (density, bulk and shear modulus, longitudinal and transversal sound velocities, and pressure) as a function of the distance from the Earth's centre are given in the Preliminary Reference Earth Model (PREM) [10], which is based on seismic observations. In the following we compare the high-temperature elastic properties of bcc Fe-Mg alloys, calculated within the present study, with seismic data of the inner core, as given in PREM [10].

It is known that the resistance of pure iron to shear does not match the very low shear modulus of the Earth's inner core [4]. At 360 GPa pressure, Belonoshko et al. calculated G=274.3 GPa at T=6000 K, and G=243.1 GPa for bcc Fe at T=7400 K [4, 30]. From seismic observations [10], the shear modulus of the inner core varies between 156.7 and 176.1 GPa. Our calculations show that 5% Mg addition at 364 GPa and T=7000 K, decreases the shear modulus of pure bcc iron to 165.83 GPa (Table 2), which is in excellent agreement with seismic data (Fig. 3, top panel). The calculated shear moduli of $Fe_{0.9}Mg_{0.1}$ T=7000 K, however, are significantly higher than those of the core, indicating that at this temperature, less Mg might be present in the core.

The bulk moduli, B, calculated for $Fe_{0.95}Mg_{0.05}$ and $Fe_{0.9}Mg_{0.1}$ alloys are shown in the middle panel of Fig. 3. The calculated B values agree well with the bulk modulus of the core for both alloys. The bulk modulus of the core is $B^{\rm PREM}$=1425.3 GPa at $P^{\rm PREM}$=364 GPa pressure [10]. For $Fe_{0.95}Mg_{0.05}$ we obtain B=1424 GPa (Table 1) at P=364 GPa pressure, which differs from

the bulk modulus of the core by -0.1%. The present calculated bulk modulus for $Fe_{0.9}Mg_{0.1}$, B=1386 GPa at P=362 GPa pressure, deviates from that of the core by -3%.

The present theoretical longitudinal sound velocities, $v_{\rm P}$, show good agreement with seismic observations for both Fe-Mg alloys (Fig. 3, bottom panel). We calculate $v_{\rm P}$=11.0 km/s at P=364 GPa pressure in $Fe_{0.95}Mg_{0.05}$ (Table 2), which differs from $v_{\rm P}^{PREM}$=11.26 km/s (at $P^{\rm PREM}$=364 GPa) by -2%. For $Fe_{0.95}Mg_{0.05}$ the calculated $v_{\rm P}$=11.4 km/s deviates from that of the core by 1%. The transversal sound velocity of the core is $v_{\rm S}^{PREM}$=3.67 km/s at $P^{\rm PREM}$=364 GPa pressure. We calculate $v_{\rm S}$=3.5 km/s at P=364 GPa in $Fe_{0.95}Mg_{0.05}$, which agrees well with that of the core, the difference being -5%. We obtain larger deviation for $Fe_{0.9}Mg_{0.1}$: $v_{\rm S}$=4.3 km/s calculated at P=362 GPa differs from that of the core by 17%.

Based on the present and our previous [12] results, we suggest that in the core, Mg has a decreasing concentration profile with increasing pressure. Namely, close to the boundary of the inner core, ≈9% Mg provides good agreement with seismic data, while in the central part of the core ≈5% Mg may be present. We note here that our results were obtained by neglecting phonon contributions. To estimate the effect of phonons, we consider Belonoshko et al.'s molecular dynamics simulations [4]. For pure bcc Fe, at P=360 GPa they calculated C'=13.8 GPa at T=6000 K and C'=26.3 GPa at T=7000 K. Assuming linear temperature dependence for elastic constants in this temperature interval, C' would be increased by about 66 GPa due to vibration in pure Fe at T=7000 K. At this temperature, and at P=364 GPa, with the phonon correction we get C'≈75 GPa, and in turn, G≈202 GPa in

$Fe_{0.95}Mg_{0.05}$. This indicates that taking into account lattice vibrations, less than 5% Mg would be enough to reproduce the physical properties of the core T=7000 K.

4. Conclusions

We presented the equation of state for pure bcc Fe and bcc Fe-Mg alloys containing 5 and 10% Mg. We found that the volume difference between Fe and Fe-Mg alloys is negligible at inner core pressures. We showed that both bcc Fe and Fe-Mg alloys are dynamically unstable at zero temperature, as their tetragonal shear modulus, C', is negative. We demonstrated that Mg significantly increases the tetragonal shear modulus of iron. This effect makes bcc Fe-Mg alloys dynamically stable at high temperature, while bcc Fe remains dynamically unstable at core pressures, even at T=7000 K. We gave an electronic structure explanation of the stabilization effect of Mg. We showed that the thermo-physical properties of bcc $Fe_{0.95}Mg_{0.05}$ are in good agreement with those of the Earth's inner core as provided by seismic observations.

Acknowledgement

The Kami Research Foundation, the Swedish Research Council, the Swedish Foundation for Strategic Research, and the Swedish Foundation for International Cooperation in Research and Higher Education are acknowledged for financial support. The calculations were performed on UPPMAX and HPC2N resources.

References

[1] W. Ross, D. A. Young, and R. Grover, J. Geophys. Res. 95 (1990) 21713.

[2] M. Matsui, and O. L. Anderson, Phys. Earth Planet. Inter. 103 (1997) 55.

[3] A. B. Belonoshko, R. Ahuja, and B. Johansson, Nature 424 (2003) 1032.

[4] A. B. Belonoshko, N. V. Skorodumova, S. Davis, and A. N. Osiptsov, Science 316 (2007) 1603.

[5] A. B. Belonoshko, N. V. Skorodumova, A. Rosengren, and B. Johansson, Science 319 (2008) 797.

[6] J. F. Lin, D. L. Heinz, A. J. Campbell, J. M. Devine, and G. Shen, Science 295 (2002) 313.

[7] B. Chen, L. Gao, K. Funakoshi, and J. Li, Proc. Nat. Acad. Sci. 104 (2007) 9162.

[8] L. Dubrovinsky, N. Dubrovinskaia, O. Narygina, I. Kantor, A. Kuznetzov, B. Prakapenka, L. Vitos, and B. Johansson, Science 316 (2007) 1880.

[9] R. Hemley, and H. K. Mao, Int. Geol. Rev. 43 (2001) 1.

[10] A. Dziewonski, and D. Anderson, Phys. Earth. Planet. Inter. 25 (1981) 297.

[11] K. Kádas, L. Vitos, and R. Ahuja, Earth Planet. Sci. Lett. 271 (2008) 221.

[12] K. Kádas, L. Vitos, B. Johansson, and R. Ahuja, Proc. Nat. Acad. Sci. 106 (2009) 15560.

[13] W. McDonough, and S.-s. Sun, Chem. Geol. 120 (1995) 223.

[14] C. Allegre, J.P. Pirier, E. Humler E, and A. Hofmann, Earth. Planet. Sci. Lett. 134 (1995) 515.

[15] R. A. Robie, B. S. Hemingway, and J. R. Fisher, U.S. Geiological Survey Bulletin, 1452 (1978).

[16] P. Hohenberg, and W. Kohn, Phys. Rev. 136 (1964) B864.

[17] J. P. Perdew, K. Burke, and M. Ernzerhof, Phys. Rev. Lett. 77 (1996) 3865.

[18] L. Vitos, H. L. Skriver, B. Johansson, and J. Kollár, Comp. Mat. Sci. 18 (2000) 24.

[19] L. Vitos, Phys. Rev. B 64 (2001) 014107.

[20] L. Vitos, I. A. Abrikosov, and B. Johansson, Phys. Rev. Lett. 87 (2001) 156401.

[21] O. K. Andersen, O. Jepsen, G. Krier, in: Lectures on Methods of Electronic Structure Calculation, World Scientific, Singapore, 1994, p. 63.

[22] L. Vitos, P. A. Korzhavyi, and B. Johansson, Nature Materials 2 (2002) 25.

[23] L. Dubrovinsky, N. Dubrovinskaia, F. Langenhorst, D. Dobson, D. Rubie, C. Gesmann, I. A. Abrikosov, B. Johansson, V. I. Baykov, L. Vitos,

T. Le Bihan, W.A. Crichton, V. Dmitriev, and H. P. Weber, Nature 422 (2003) 58.

[24] K. Kádas, L. Vitos, and R. Ahuja, Appl. Phys. Lett. 92 (2008) 052505.

[25] K. Kádas, L. Vitos, B. Johansson, and J. Kollár, Phys. Rev. B 75 (2007) 035132.

[26] L. Huang, L. Vitos, S. K. Kwon, B. Johansson, and R. Ahuja, Phys. Rev. B 73 (2006) 104203.

[27] N. Dubrovinskaia, L. Dubrovinsky, I. Kantor, W. A. Crichton, V. Dmitriev, V. Prakapenka, G. Shen, L. Vitos, R. Ahuja, B. Johansson, and I.A. Abrikosov, Phys. Rev. Lett. 95 (2005) 245502.

[28] G. Grimvall, Thermophysical Properties of Materials, enlarged and revised edition (North-Holland, Amsterdam, 1999).

[29] Z. Hashin, and S. Shtrikman, J. Mech. Phys. Solids 10 (1962) 343.

[30] A. B. Belonoshko, R. Ahuja, and B. Johansson, Phys. Rev. Lett. 84 (2000) 3638.

Figure captions

Figure 1: Calculated equation of state for nonmagnetic (NM) and ferromagnetic (FM) pure bcc Fe (denoted by black circles and red squares, respectively), NM bcc $Fe_{0.95}Mg_{0.05}$ (red base-down triangles), and bcc $Fe_{0.9}Mg_{0.1}$ alloys (blue base-up triangles).

Figure 2: Electronic density of states of nondistorted (δ=0, solid lines) and distorted (δ=0.05, dashed lines) bcc Fe (black curves) and $Fe_{0.9}Mg_{0.1}$ (red curves) around $E_{\rm F}$, at V=44.60 Bohr^3/atom volume at zero temperature. The Fermi level is denoted by the vertical dashed line.

Figure 3: Shear (G) and bulk moduli (B), longitudinal ($v_{\rm P}$) and transversal ($v_{\rm S}$) sound velocities of bcc $Fe_{0.95}Mg_{0.05}$ (red circles) and $Fe_{0.9}Mg_{0.1}$ alloys (black squares) at T=7000 K temperature. For comparison, seismic data as given in PREM [10] are also displayed (blue triangles).

Table 1: Elastic constants, C', C_{44}, and the bulk modulus, B, at different V volumes, calculated for pure bcc Fe, bcc $Fe_{0.95}Mg_{0.05}$ and bcc $Fe_{0.9}Mg_{0.1}$ alloys at T=0 K, and at T=7000 K. C', C_{44}, and B are given in GPa, V is in Bohr^3/atom.

	Fe			$Fe_{0.95}Mg_{0.05}$			$Fe_{0.9}Mg_{0.1}$		
V	C'	C_{44}	B	C'	C_{44}	B	C'	C_{44}	B
T=0 K:									
44.60	-285.3	772.0	1447	-172.0	721.3	1405	-83.4	668.8	1370
47.71	-253.5	662.8	1177	-159.8	614.3	1149	-78.5	570.6	1126
50.97	-228.6	565.2	954	-145.2	522.0	936	-70.9	487.6	922
54.36	-205.6	478.9	769	-130.5	442.7	759	-64.4	414.3	752
57.91	-183.5	406.2	616	-118.0	374.7	612	-60.2	352.0	610
T=7000 K:									
44.60	-43.7	681.6	1464	8.8	648.8	1424	55.1	618.6	1386
47.71	-23.7	571.9	1190	17.7	547.6	1164	54.8	525.2	1139
50.97	-8.1	478.9	964	25.5	462.5	948	53.3	444.6	932
54.36	4.0	401.4	778	30.0	389.2	769	51.8	377.4	760
57.91	11.5	335.0	625	30.4	326.2	621	46.6	318.5	618

Table 2: Shear (G) and Young (E) moduli, polycrystal anisotropy ($A = (G_{\rm V} - G_{\rm R})/(G_{\rm V} + G_{\rm R})$, see text for details), longitudinal ($v_{\rm P}$) and transversal ($v_{\rm S}$) sound velocities calculated for bcc $Fe_{0.95}Mg_{0.05}$ and $Fe_{0.9}Mg_{0.1}$ alloys at different V volumes, at T=7000 K. Shear and Young moduli are given in GPa, sound velocities are in km/s, and V is in Bohr^3/atom.

	$Fe_{0.95}Mg_{0.05}$					$Fe_{0.9}Mg_{0.1}$				
V	G	E	A	$v_{\rm P}$	$v_{\rm S}$	G	E	A	$v_{\rm P}$	$v_{\rm S}$
44.60	165.8	478.9	0.90	11.0	3.5	247.9	701.8	0.53	11.4	4.3
47.71	163.4	468.2	0.78	10.4	3.6	222.0	625.3	0.48	10.8	4.2
50.97	158.7	450.8	0.66	9.9	3.6	197.3	552.8	0.44	10.2	4.1
54.36	148.0	417.2	0.57	9.3	3.6	175.6	489.2	0.39	9.6	4.0
57.91	132.2	370.2	0.51	8.7	3.6	151.7	420.7	0.37	9.0	3.9

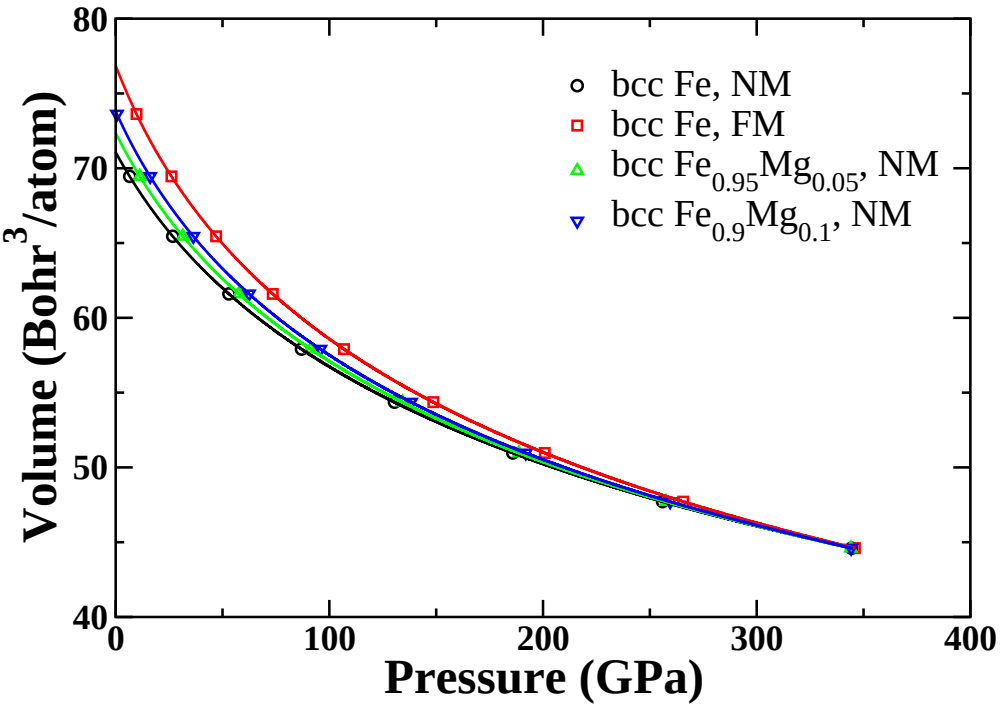
80
70
60
50
40
0
100
200
300
400
Volume (Bohr^3/atom)
Pressure (GPa)
bcc Fe, NM
bcc Fe, FM
bcc $Fe_{0.95}Mg_{0.05}$, NM
bcc $Fe_{0.9}Mg_{0.1}$, NM

Figure 1:

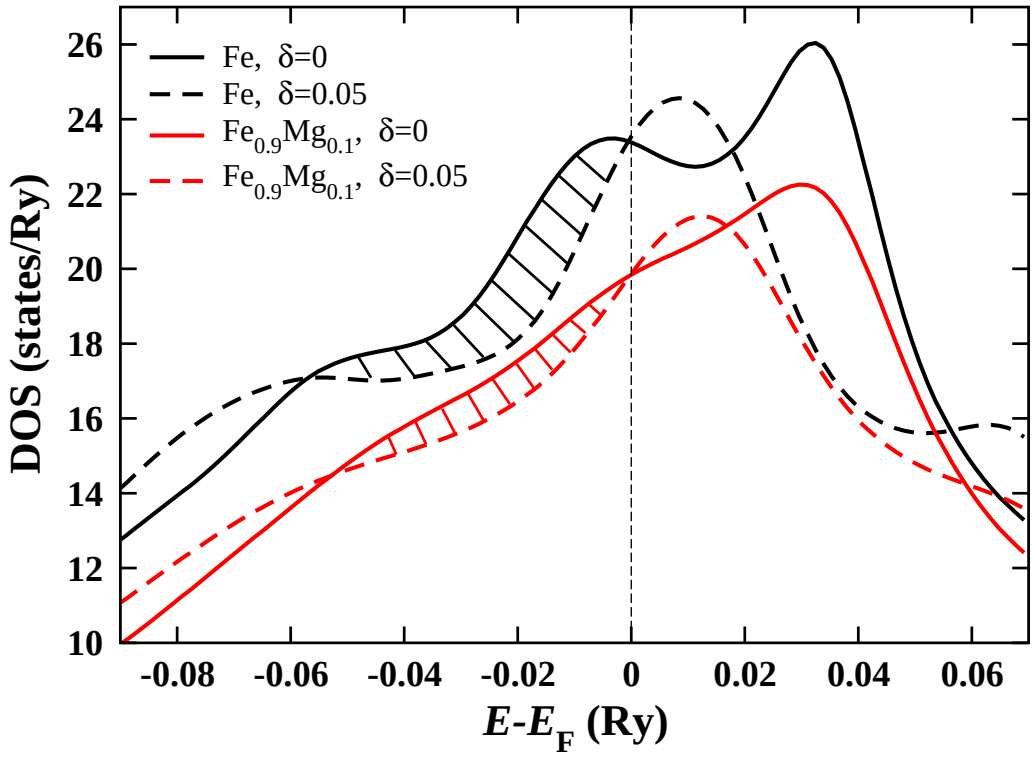
Fe, δ=0
Fe, δ=0.05
Fe0.9Mg0.1, δ=0
Fe0.9Mg0.1, δ=0.05
DOS (states/Ry)
E-EF (Ry)
26
24
22
20
18
16
14
12
10
-0.08
-0.06
-0.04
-0.02
0
0.02
0.04
0.06

Figure 2:

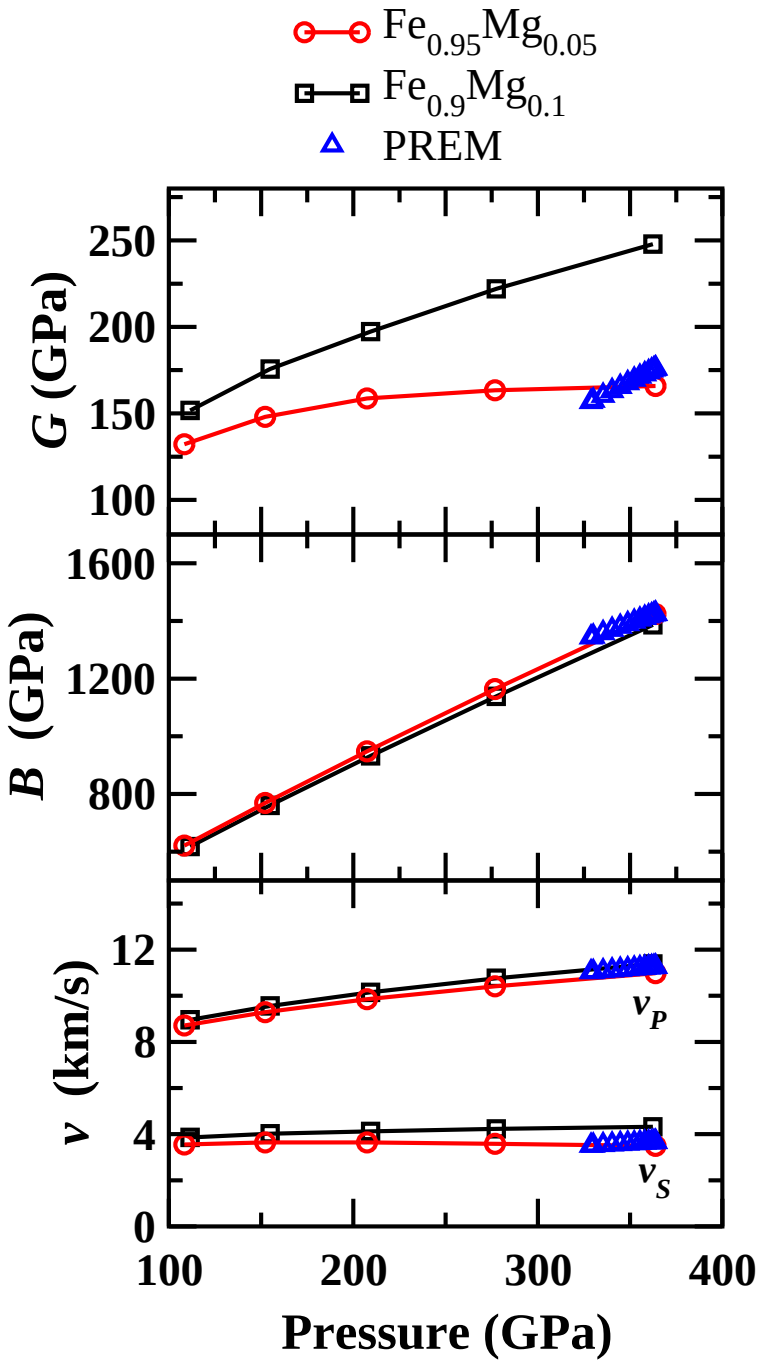
Fe0.95Mg0.05
Fe0.9Mg0.1
PREM
G (GPa)
250
200
150
100
B (GPa)
1600
1200
800
v (km/s)
12
8
4
0
vP
vS
100
200
300
400
Pressure (GPa)

Figure 3: